Journal of Engineering and Computer Sciences
Qassim University, Vol. 6, No. 1, pp. 51-74 (January 2013/Safar 1434H)

Self-excited vibration arising from tribology-dynamic interaction

H. A. Sherif and Abdelraheim, A.E.

College of Engineering, Qassim University, Saudi Arabia

Tel. (966) 541250589,P.O. Box 6677,Buraidah 51452,SA.

hasherif@qec.edu.sa

(Received 21/2/2013; accepted for publication12/5/2013)

Abstract. An elastic contact model of a pad/disc system is developed which can give some explanations on self-excited vibration induced during continuous dry friction. Based on this model, it is possible to show that establishement and sustainability of self-excited vibration in disc brake system are linked to the interface properties as well as the physical properties of the disc brake components. It is shown using theoretical and experimental analysis that the regime of self-excited vibrations can be triggered when approaching any of the modified resonant frequencies of either pad or disc system. These frequencies are dependant upon contact stiffness value during self-excitation regime. Experimental investigations have also shown that contact stiffness during sustained self-excitation may increase monotonically upto 35% of its initial value due to continuous wear and sliding. One of the main findings in this work, is that the resonance of any of the system frequencies is linked mainly to the established value of contact stiffness due to wear, load and speed. Also, for each self-excited regime, there is a limiting frequency after which the self-excited regime either sustains at this frequency or change to another regime. Sudden changing of load or speed at this limiting frequency may cause the transition from one regime of self-excitation to another.

Keywords*:* self-excited vibration, squeal noise, frequency response, contact stiffness, friction pad, disc brake

List of Symbols

A	apparent area of contact
A', B', C', D'	arbitrary constants
a, b	disc outer and inner radii
c_d, c_p	damping coefficients in disc and pad systems, respectively
d	separation between surfaces of pad and disc
E_d,E_p	Young's modulus of the disc and pad, respectively
E	effective modulus of elasticity (N/m^2)

f_{li}	limiting frequency at mode i
f_{si}	modified frequency of flexural mode i
G_{pp}	pad receptance (displacment at pad contact point with disc due to a force at this point on the pad)
Gpd	pad receptance (displacment at pad contact point with disc due to a force at this point on the disc)
h	non-dimensional separation (d/σ)
Hd	disc receptance
Hp	pad receptance
Ki	normal stiffness of a single asperity
Ke	effective normal contact stiffness of pad/disc assembly
kp	pad spring stiffness
m	mass per unit area of the plate
mp	mass of pad
n	number of contacts
s	normalized coordinate (height/σ)
t	disc thickness
W	normal load (N)
β	effective radius of asperities
η	density of asperities per unit area
	standard deviation of height distribution of asperities
$\phi^*(s)$	height distribution of asperities scaled to make its standard deviation unity
ω	disc rotational speed
Ω	excitation angular frequency
ξ	dimensionless radius

1. Introduction

The determination of the contribution of brake components in squeal generation has been of a great concern since its early appearance in last decades to suppress or eliminate brake noise [1-4]. Many independent studies have been provided by dynamicists [5-11] and tribologists [12-16] to determine the system behavior and the mechanism of self-excitation. Besides, considerable efforts have been directed to explain different friction models [17-21]. In experimental observations, many researchers have noticed that many squeal frequencies typically line up with one or more disc modal frequencies [22,23]. Self–excited vibration has been studied in the direction of surface properties relationship to the emmitted noise [24-28]. It is belived that the elastic properties of contacting surfaces play a major role in establishing system's self-excitation. Sensitivity to variations in contact parameters has also been considered [28-36] in order to determine how many modes of the disc /brake system are needed to fully predict system behavior over a limited frequency range.The present work shows that system unstable modes are represented by modified disc and pad resonances by the virtue of contact stiffness. This contact stiffness couples the pad/disc elements. The term contact stiffness is mentioned in many papers [37-38] and explained in detail in reference [39].

2. Simplified mathematical model of pad/disc system

Consider that both the pad and the disc are brought into flat contact at n spots (contact asperities) as shown in Fig. (1), under the following assumptions:

1. All asperity summits are identical.

2. Every two encountered asperities are modeled by a linear elastic spring of stiffnes K_i in normal direction of contact.

3. Disc and the pad are connected through a set of linear springs K_i (i=1,2,…,n), to form the pad/disc system as shown in Fig. (2).

4. All contact asperities can be represented by an equivalent spring stiffness K_e where:

$$K_e = \sum_{i=1}^{n} K_i \tag{1}$$

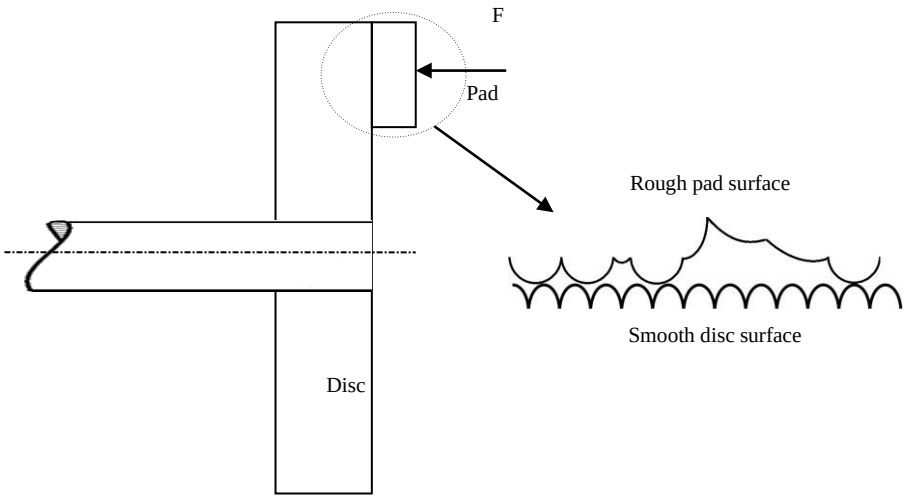

Fig. (1). Pad/disc assembly

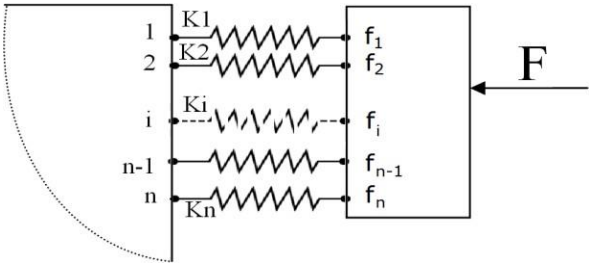

Fig. (2). Contact Model of Friction Pad With Disc

An expression for the total normal static contact stiffness K_e of two nominally flat surfaces has been given for the first time by Thomas and Sayles [36]. Detailed parameteric study of contact stiffness of nominally flat surfaces is given in [37, 39].

For simplicity, the component displacements at contact interface are considered in one direction and at one point. Applying a virtual force F to coordinate $X_{p,}$ see Fig. (3), the displacement at the two coordinates in the unassembled model in Fig. (4) can be written as:

$$x_p = H_P f_p \quad , x_d = H_d f_d \tag{2}$$

Where x_p , x_d are the pad and disc displacements at contact point, respectively. H_p and H_d are the receptances of the pad and disc before assembly.

The equilibrium condition for the components is given as:

$$F = f_p + f_d \quad \text{or}$$

$$f_p = F - f_d \tag{3}$$

The compatibility conditions can be written as:

$$f_d = k_e(x_p - x_d) \tag{4}$$

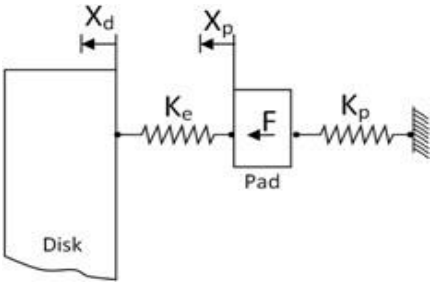

Fig. (3). Simple mathematical model of disc/pad assembly.

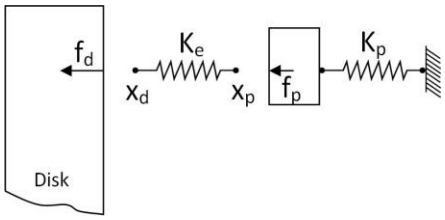

Fig. (4). Unassembled disc/pad system.

Substituting Eqns. (2) and (3) into (4), it results:

$$f_d = -\frac{x_d}{H_d} = \left[H_d + H_p + \frac{1}{k_e} \right]^{-1} H_p F \tag{5}$$

The transfer receptance (i.e. displacement x_d at contact point with the disc due to virtual force F at the pad) is given from (5) as:

$$G_{pd}(\Omega) = -\frac{x_d}{F} = H_d \left[H_p + H_d + \frac{1}{k_e} \right]^{-1} H_p$$

In a similar way, the substitution of (5) into (3) gives:

$$f_p = \frac{x_p}{H_p} = \left[1 - \left[H_d + H_p + \frac{1}{k_e}\right]^{-1} H_p\right] F_p \quad (6)$$

So, the point receptance (i.e. displacement x_p at contact point with the pad due to virtual force F at the same point) is:

$$G_{pp}(\Omega) = \frac{x_p}{F} = H_p \left[1 - \left[H_d + H_p + \frac{1}{k_e}\right]^{-1} H_p\right] \quad (7)$$

If the pad is represented by a spring-mass-damper system, then its receptance is given as:

$$H_p = \frac{1}{k_p - m_p \Omega^2 + j\Omega c_p} \quad (8)$$

The disc response can be written as [40]:

$$H_d = \sum_{i=1}^{n} \frac{\xi_0 Z_i(\xi_0) Z_i(\xi)}{(\omega_{id}^2 - \Omega^2 + j\Omega c_d) ma N_{ii}} \quad (9)$$

Where

$$\omega_{id}^2 = \frac{\lambda_i^4}{ma^4}$$

$$Z_i(\xi) = A' J_0(\lambda_i \xi) + B' Y_0(\lambda_i \xi) + C' I_0(\lambda_i \xi) + D' K_0(\lambda_i \xi)$$

$$N_{ii} = \int_0^1 \xi Z_i(\lambda_i \xi) Z_i(\lambda_i \xi) d\xi$$

Where $J_0(\lambda_i \xi)$ is Bessel function of the 1st kind, integral order 0

$Y_0(\lambda_i \xi)$ is Bessel function of the 2st kind, integral order 0

$I_0(\lambda_i \xi)$ is Modified Bessel function of the 1st kind, integral order 0

$K_0(\lambda_i \xi)$ is Modified Bessel function of the 2st kind, integral order 0

Equations (6) or (7) present a simple form of the tribology-dynamic interacrtion in terms of the contact stiffness and response of pad/disc system components. However, it is not simple to depict this interaction because the solution of either equation is not straightforward. Separation of real and imaginary parts of the receptance G(Ω) in either equation enables the analysis of the contribution of contact stiffness and system parameters on system receptance. The solution of Eq. (9) and then (7) or (8) can be simply obtained using the finite element appraoch.

3. Numerical Analysis

FEM is used to obtain the receptances H_d of fixed-free disc and H_p of simply supported friction pad. Using these results it will possible to get the receptance of the combined system (Pad/disc). A FEM representation for the pad/disc assembly is shown in Fig. (5). The model was built using the solid modeling. Two volumes had been created, the first one is an annular disc and the second is the pad sector. No asymmetric analysis is considered in this modeling. The model of the Grey Cast Iron disc (E_d=2.1x10^{11}N/m^2, ρ_d=7860kg/m^3) with inner radius b=75 mm, outer radius a=150 mm and thickness t=9mm, contains 2304 nodes and 1080 elements. The disc is modeled as completely fixed from the neck while its outer edge is free. The model of the pad sector (E_p=10^9 N/m^2, ρ_p=650 kg/m^3) with inner radius=105 mm and outer radius=145 mm, sector angle=50˚ and thickness b=15mm, contains 198 nodes and 80 elements. The pad is modeled as it is pivoted from its back by a set of linear springs. The springs are fixed from the other ends in the three directions. Each node of the pad –in the side facing the disc- is connected to its corresponding disc-node by a contact spring.

A 3-D point-to-surface contact element is used. The element is a five node element and has three linear degrees of freedom. Each set contains 7920 elements. The set of the elements that support the pad to the fixed support has total stiffness of 5x10^4 N/m while the stiffness of the contact set between the pad and the disc is varying from 10^5 N/m to 10^9 N/m in a parametric study fashion. Four flexural modes (diametric modes) of this model are shown in Fig. (6) with their frequencies at K_e=10 MN/m.

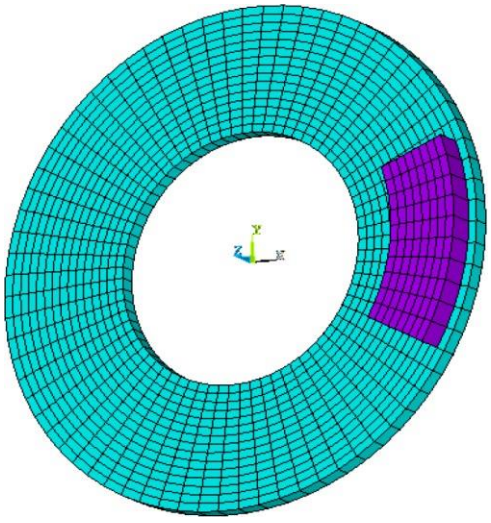

Fig. (5). FEM of pad/disc assembly

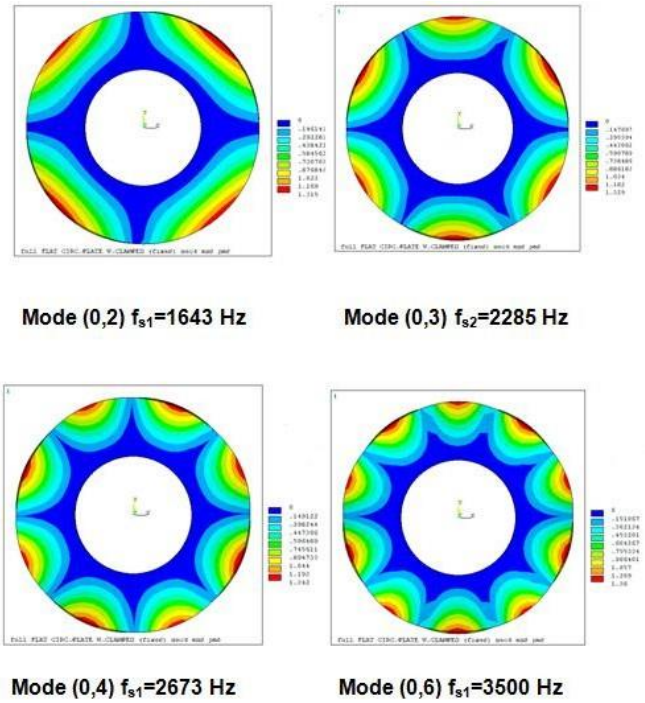

Fig. (6). Disc flexural modes (K_e=10MN/m)

Using this model, it is possible to show the effect of coupling between pad and disc surfaces due to contact stiffness K_e. Beside, the analysis provides the system resonance frequencies f_{si} as well as disc natural frequencies f_{id}. Using these data it is possible to make a parametric study of the effect of contact stiffness and physical characteristics of the pad/disc assembly on the system receptance using Eq. (6).

The disc receptance H_d is shown in Fig. (7), while the system response G_{pp} at different values of contact stiffness is given in Fig. (8). It is observed that the frequencies of flexural (diametric) modes monotonically increase with the contact stiffness K_e while the frequencies of other modes (e.g. extensional, torsional modes,..) do not change much with contact stiffness. The system response (receptance G_{pp}) within the range of two extreme values of contact stiffness (70-100 MN/m) at the point of contact, shows an expected slight shift of the frequencies of flexural modes. For example, flexural modes increased from 1643, 2150 and 2673Hz at K_e=70 MN/m to 1678, 2285 and 2778Hz at K_e=100 MN/m. On the other hand, the last two freqencies (6150 Hz and 7200 Hz) are significantly affected by the increase of K_e. These two frequencies represent the translational modes of the pad as a mass-spring system coupled with the mass of the disc by contact stiffness K_e.

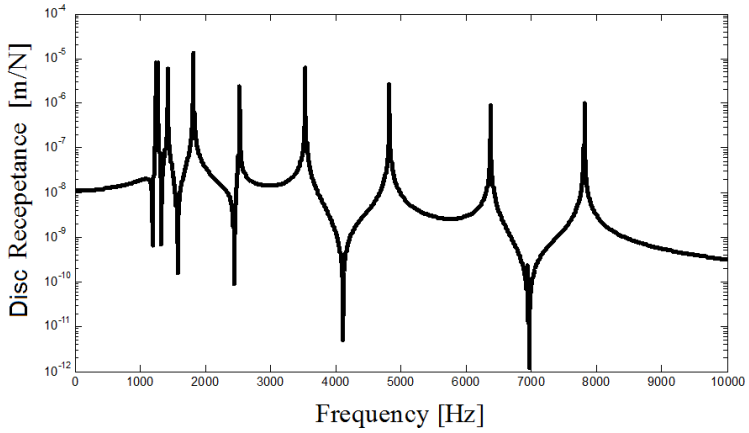

Fig. (7). Receptance H_d of fixed-free disc.

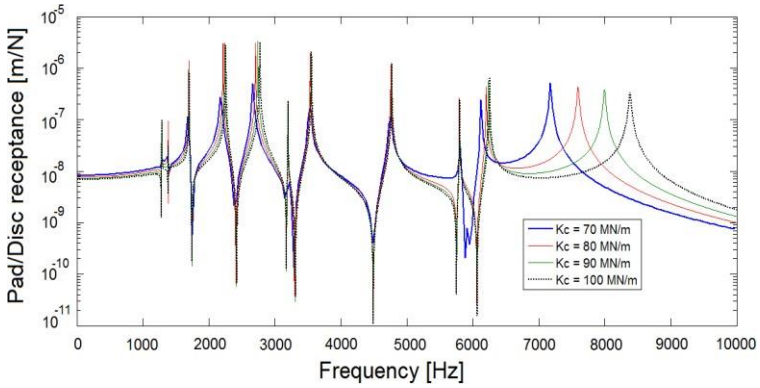

Fig. (8). Receptance G_{pp} of pad/disk system

With the increase of contact stiffness, all the system flexural frequencies approach constant values sooner or later (frequency limit) according to their order (Fig. (9)), while the higher translational frequency keeps increasing and the lower one approaches a constant value with the increase in the contact stiffness. For example, the limiting frequencies for flexural modes f_{s1} , f_{s3} and f_{s2} from Fig. (9) are f_{l1}= 1678, f_{l2}=2400 and f_{l3}= 2900 Hz. This means that these three flexural frequencies stop increasing beyond correspondant values of contact stiffness K_e=80, 120 and 150 MN/m, respectively.

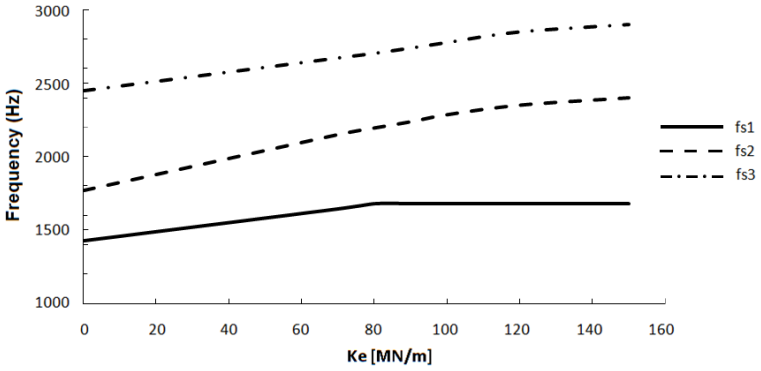

Fig. (9). Variation of frequency of flexural modes f_{s1}, f_{s2}, f_{s3} with contact stiffness

4. Experimental measurements

To investigate the effect of contact stiffness on the system dynamic response as well as the self-excited modes, two main experiments are conducted. The first one is a shock test where the effect of contact stiffness on system response is investigated at different applied normal load and no sliding speed. The second test depicts the system response during self-excited regimes at different applied loads and speeds. In the two cases, the measurement of disc response is needed to recognize the effect of contact on its modal frequencies.

The adopted model of pad/disc system (Fig. (10)) consists of a cubic friction pad in contact with a plexiglass disc with inner radius 50 mm, outer radius 150 mm and thickness 20 mm. The pad dimensions is selected to fulfill a model of rigid body in contact with an elastic disc. The disc is rotated by a variable speed motor with speed range from 0 to 200 rpm. The normal load acted on the back plate of the friction pad through a steel ball, is produced by dead weight on a pulley rope system. The pad is supported from one side by an elastic leaf spring resisting its motion in tangential direction of contact with the disc to form a mass-spring model. The pad and its back plate are mounted in an antifriction slider to enable the horizontal and vertical adjustment of the contact position with the disc and to ensure the pad/disc flat contact even if there is a disc runout. Low range of disc speed (up to 60 rpm) is used to eliminate the effect of disc rotation on its resonance frequencies and to avoid the temperature rise due to friction.

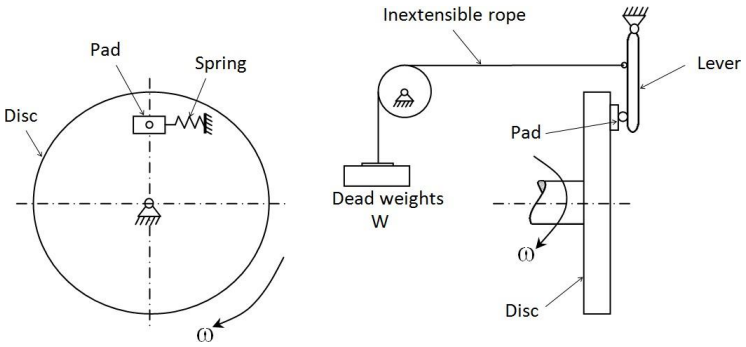

Fig. (10). Experimental model

4.1 Measurement of disc frequency response

Impact hammer with a force transducer mounted on its tip is used to measure the accelerance (acceleration/force) of the clamped-free disc. The very light piezoelectric accelerometer (0.7 gm) having frequency range up to 20 kHz is fixed on the surface of the disc mounted in the test stand as shown in Fig. (11). The slight lateral hammering of the disc is made at different points laying on the contact circle of the pad location with the disc (at a line making 90°, 60° and 45° with the diammetral passing through the point of fixation of the accelerometer) to extract all possible frequencies of lateral vibration of the disc. Zoom measurement is used for achieving greater frequency resolution in the determination of the resonance frequency for each mode.

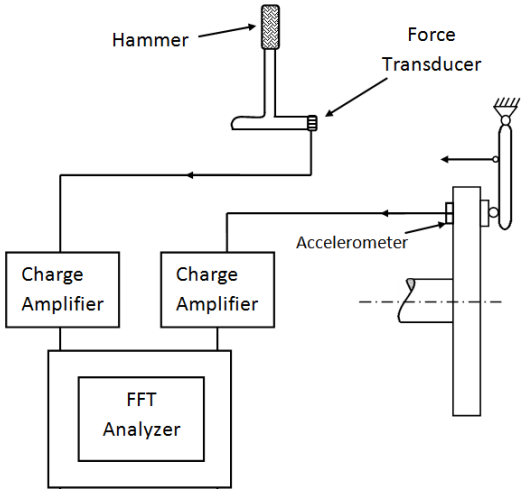

Fig. (11). Measurement of disc and system (pad/disc) receptance

For example, Fig. (12) shows the frequency response curves of the disc when it is hammered at point of intersection of the contact circle with a line making 60° with the diammetral passing through the point of fixation of the accelerometer. According to these measurement, the resonance frequencies of the disc flexural modes are 550, 880, 3500, 5170, 7100, 9320, and 11890 Hz.

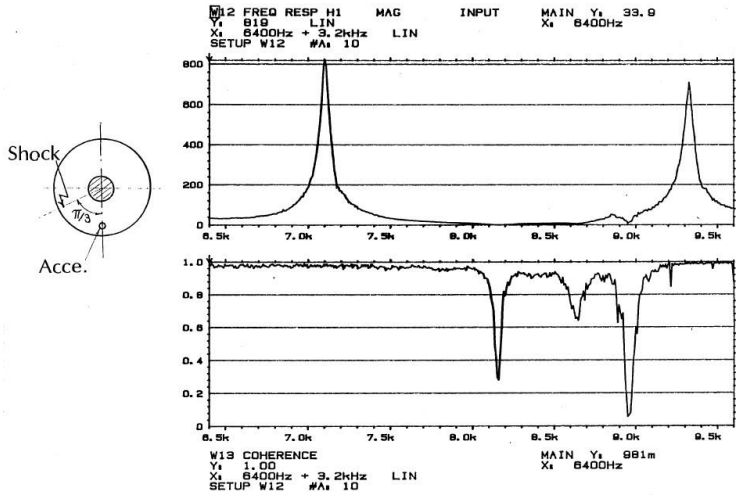

Fig. (12). Sample of zoomed measured disc receptance (flexural modes)

4.2 Investigation of tribology-dynamic interaction in pad/disc assembly

To show the effect of contact stiffness on the system response, a series of receptance shock tests are conducted under different applied normal loads. These tests show the effect of contact stiffness on system response without relative motion between contact surfaces. A cubic friction pad (type F-153 Valeo) with rough intact surface is brought into contact with the smooth surface of a plexiglass disc. Plexiglass disc is used to easily get to the surface conditions for a self-excited pad/disc combination. Using a plexiglass disc makes it easy to establish self-excitation under relatively medium operating conditions. Under such surface conditions and according to the analysis developed in [27,28], the normal contact stiffness value is expected to be very low.

The very light accelerometer is fixed on the back of the disc surface. The system frequency response is obtained using the impact hammering (shock technique) of the non-rotating disc in a direction normal to its surface at position paralell to its contact with the pad. Fig. (13) shows the frequency spectra of the static system within a range from 0 to 13 kHz at different applied normal load for a cubic friction pad (25x25x10 mm) having square area of contact = 6.25 cm^2. As a matter of fact, there are many flexural frequencies in Fig. (13) which are modified with normal load. To investigate the tribology-dynamic interaction within this range of frequency, it is better

to focus only on the two flexural modes with frequencies f_{s1} and f_{s2} that are clearly affected by the increase of normal load. However, to identify the flexural mode, one must use the disc response curve. Inspection of these two responses revealed that flexural disc modes 5170 Hz and 7100 Hz are modified by the virtue of contact stiffness at W=20 N to modes at 5700 Hz and 8690 Hz , respectively. The shifting of these frequencies with the applied normal load can be seen from the set of displayed curves in Fig. (13) where the flexural modes f_{s1} and f_{s2} are shifted from 5700 and 8690 Hz at W=20 N to 6100 Hz and 8960Hz at W=100 N, respectively.

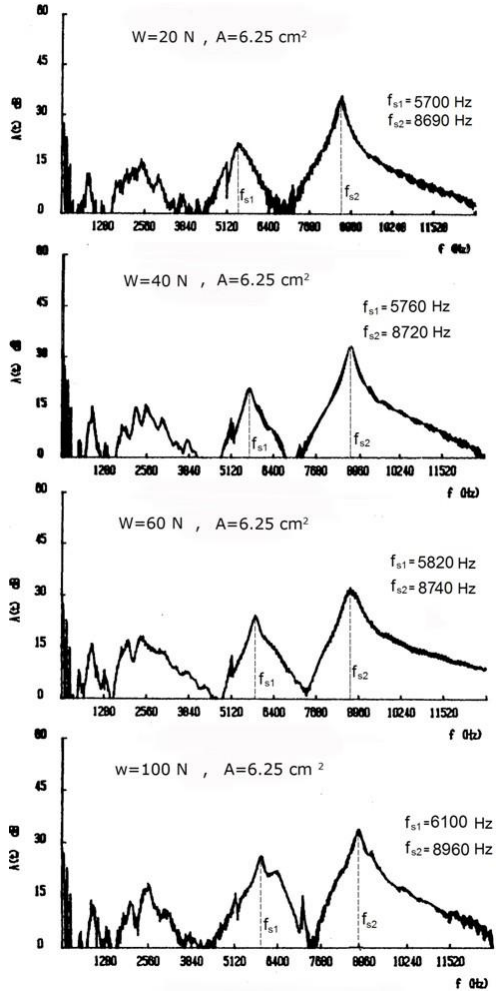

Fig. (13). Effect of applied normal load W on the pad/disc system response with zero relative velocity (contact area A=6.25 cm^2).

4.3 Estimation of contact stiffness value from measured system response

The calculations of contact stiffness from the measured responses in Fig. (13) require the substitution of modal parameters (frequencies, modal masses, modal damping) from the measured response of the fixed-free disc into Eq.(6) with assumed values of K_e that may lead to a complete matching between both measured and reconstructed responses. Fig. (14) gives an example for such reconstruction to demonstrate the modification of disc modes by contact with the pad.

The set of response curves reconstructed from response data (e.g. Fig. 13) and Fig. (14) using Eq. (6) are plotted with a suitable magnification in Fig. (15) to show relation between applied load W, contact stiffness K_e and frequencies of flexural modes f_{s1} and f_{s2}.

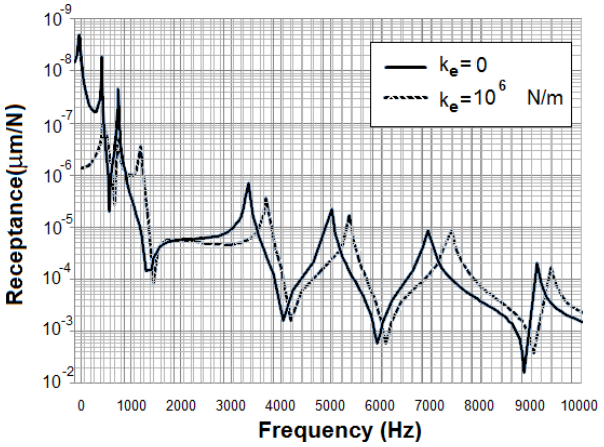

Fig. (14). Reconstructed receptances of pad/disc system from experimental data

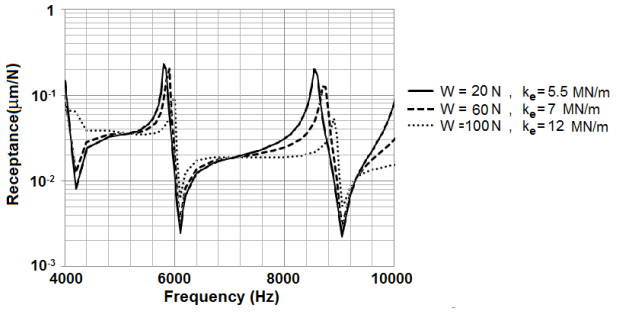

Fig. (15). Estimated contact stiffness from reconstructed system response at different normal loads (A=6.25 cm^2)

5. Parametric analysis

To show the effect of contact area on contact stiffness, another cubic friction pad (32x32x10 mm) with contact area=10.24 cm^2 is used in the above testing under the same conditions. When repeating the experiment with this pad, a similar trend of system response with the normal load has been obtained as shown in Fig. (16). The two investigated frequencies f_{s1} and f_{s2} increase with the applied normal load from 5250 and 8550 Hz at W=10 N to 5880 and 8850Hz at W=100 N, respectively.

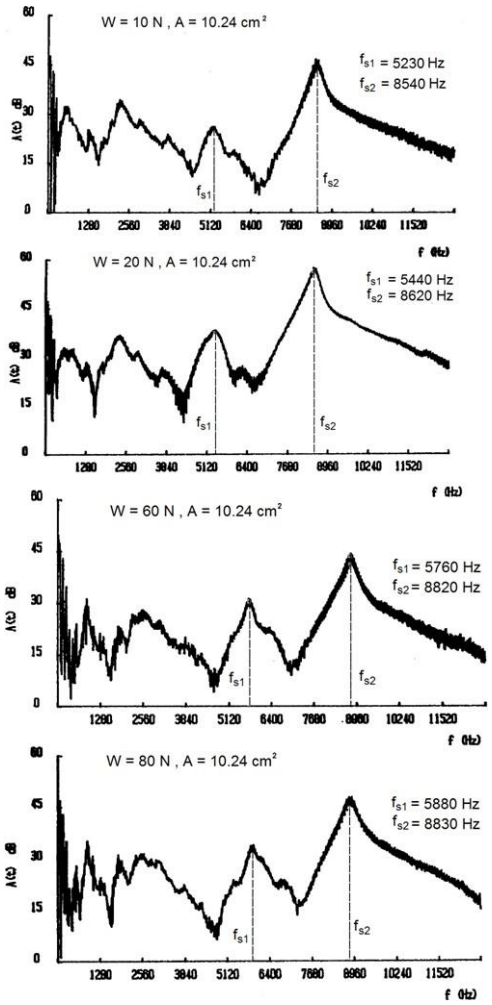

Fig. (16). Effect of applied normal load W on the pad/disc system response with zero relative velocity (contact area A=10.24 cm^2).

Fig. (17) shows the variation of the estimated contact stiffness with normal load for the two different areas of contact using Eq.(6).

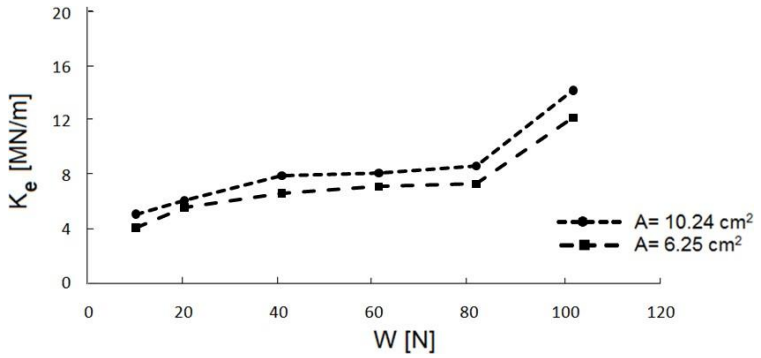

Fig. (17). Effect of contact area on the estimated contact stiffness (ω=0)

To show the effect of contact stiffness on the establishment and sustainability of system self-excitation, both system vibration and noise level are measured. The light accelerometer is mounted on the back of the friction pad in normal direction of contact with the disc to measure the system frequency spectrum when self-excited vibration (squeal) is generated. A microphone is fixed in front of the disc and in normal direction to its surface at a distance of about 10 cm to measure the sound pressure level of squeal noise. Output signals from the accelerometer and the microphone are entered into the FFT analyzer input terminals in order to check the coincidence of the two measured spectra. The squeal frequency spectra are recorded when the disc is rotating at different speeds and normal loads.

At the moment of squeal triggering, one of the investigated instantaneous self-excited system frequency f_s is 7904 Hz. This frequency increases from 7904 Hz at normal load W=50 N to 8352 Hz at W=80 N as shown in Fig. (18). This variation corresponds to a change of contact stiffness from 2.5 MN/m at 7904Hz to 4.2 MN/m at 8352Hz. The established unstable mode can be changed by either changing the applied load or the rubbing speed. When repeating the same experiment later at the same speed, the self-excited squeal triggered at normal load W=80N with another lower frequency of 4688 Hz.

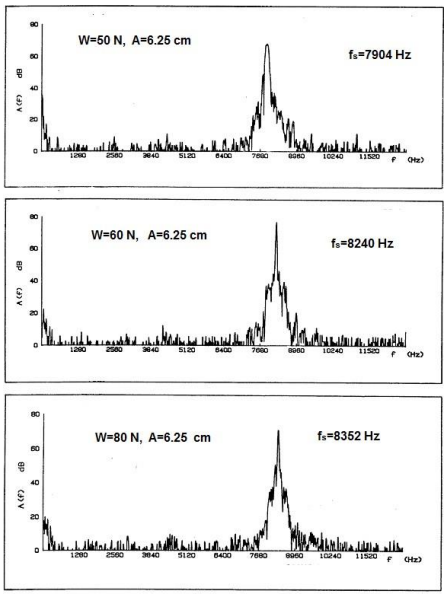

Fig. (18). Effect of applied normal load on the self-excited squeal frequency (ω=45 rpm)

According to Eq.(6), the resonance of any of the system frequency is linked mainly to the created value of contact stiffness by wear, load and speed. This can be explained using Fig. (19) as follows: any of self-excited vibration modes (point a, b,c..) can be triggered at contact stiffness K^* depending on the input excitation frequency which is function of the applied normal force, speed and interface properties. The frequency of self-excited vibration f_{s1} at point a will move in the direction aa' due to the increase of contact stiffness K^*.

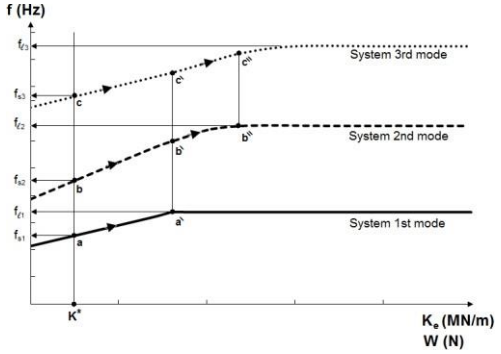

Fig. (19). Variation of squeal and limiting frequencies with load and normal stiffness at all system flexural modes

This increase in K* is related to the increase of load W or the variation of interface properties. If f_{s1} reached the limiting frequency fl_1 (i.e. point a moved to a'), there are two probable situations; the first one is that squeal with frequency fl_1 sustains, the second one is that squeal at another system mode triggers (i.e. point a' moves to b' or c" or…). Establishment of squeal means that points a, b, c… do not move and K* keeps its value to the next occurrence of wear of sliding surface to create another value K**. Similarly, frequency attained at b' can move in the direction bb' until reaching limiting frequency fl_2 and squeal either sustains at point b' or triggers at another frequency c". All other system modes follow the same previous mechanism.

To determine the effect of load and speed on the limiting frequency at this mode, the variation of squeal frequencies due to continuous rubbing under different operating conditions at the 5th modified disc frequency (7100 Hz) has been investigated as shown in Fig. (20). In this investigation, the measured squeal frequencies are recorded within load range from 20 to 80 N with step 20 N at three different rotating speed ω = 10, 20, 50 rpm . These results depict the trend of variation of squeal frequencies-by the virtue of contact stiffness variation with the normal load at different relative velocities. According to these curves, one can simply deduce that the values of the limiting frequency f_l at each speed 10,20 and 50 rpm are 9300, 9170 and 9100 Hz, respectively. By substituting the frequency data from this investigation into Eq(6), it is possible to plot the relation between applied normal load and contact stiffness at different sliding speed as shown in Fig. (21).

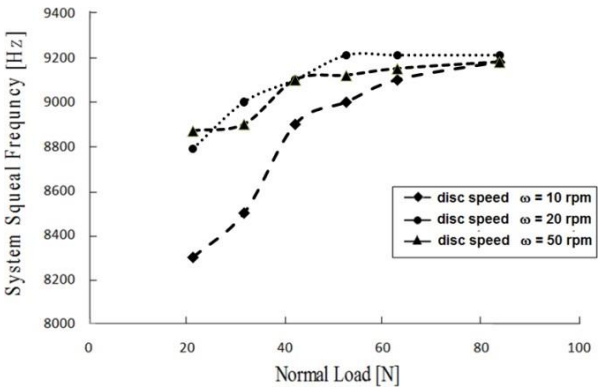

Fig. (20). Variation of the established squeal frequency due to continuous sliding at different operating conditions

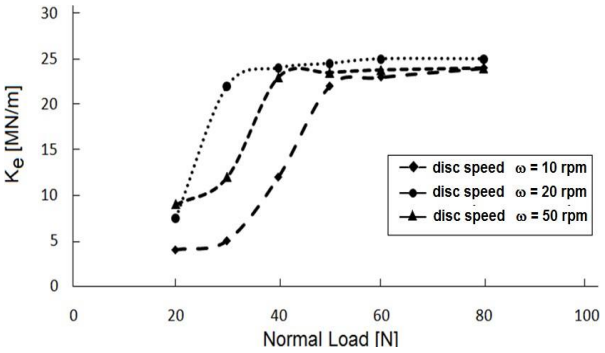

Fig. (21). Variation of the estimated contact stiffness with operating conditions

After a relatively long time of continuous rubbing (about 3-4 min.) under constant load and speed between pad and disc surfaces, self-excited squeal changes its frequency within a relatively wide band which depends on the development of the contact stiffness by wear only. Squeal is averaged within this period of time to show the change of squeal frequency from 10.496 kHz to 11.296 kHz as shown in Fig. (22). This change corresponds to an increase of contact stiffness from 6.4 MN/m to 8.63 MN/m. At higher flexural modes, this band width increases as shown in Fig. (23) where the squeal frequency is firstly established at 12.16 kHz and continued to increase to 13.16kHz during about 3 minutes of continuous sliding friction (band width=1kHz) . The band width may be shorter or wider depending on these applied operating conditions.

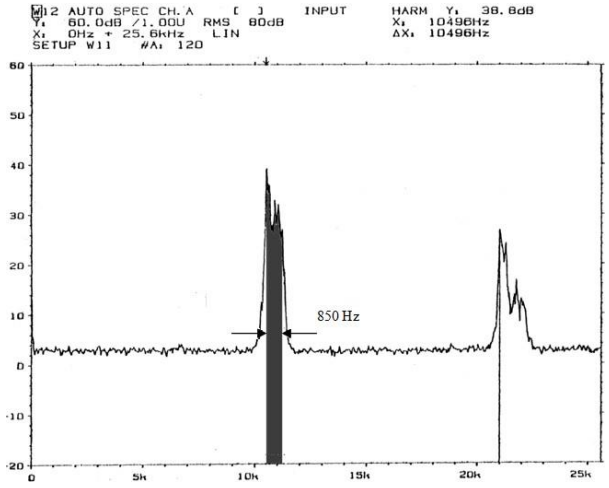

Fig. (22). Change of squeal frequency due to continuous wear and rubbing (W=80 N)

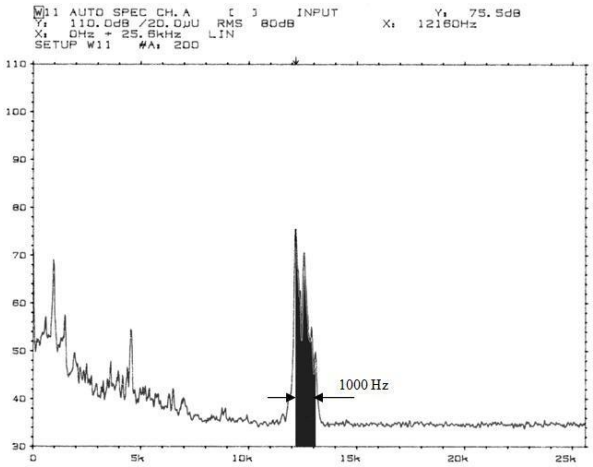

Fig. (23). Change of squeal frequency due to continuous wear and rubbing (W=120 N)

6. Conclusions

A mathematical model for describing the tribology-dynamic interaction in pad/disc system as a function of contact stiffness and system response is thoroughly explained. The developed model enables the estimation of contact stiffness from the measured response of pad/disc system. Theoretical and experimental investigations revealed the effect of contact stiffness on the modification of both disc and pad frequencies in terms of applied normal load and sliding speed. Using the experimental model, it was possible to show the direct dependance of contact stiffness on the normal load as general theory states [29,31]. According to the developed model, self excitation of pad/disc system can be established at any of the system flexural frequencies due to the variation of contact stiffness with dynamic operating conditions (load and speed). When the excitation frequency approaches any of pad/disc system modified frequencies (i.e. disc modal frequencies modified by contact stiffness), self-excited vibration with the corresponding frequency is triggered. This frequency never coincides with either disc or pad vibrational frequencies due to presence of contact stiffness. In other words, different squeal regimes occur at frequencies close but not coincident to the resonant frequencies of either pad or disc due to contact stiffness variation. Unstable vibration sustainability depends on the persistence of the value of contact stiffness. Continuous rubbing of contact surfaces modifies contact stiffness value which may in turn lead to the variation of the frequency of self-excited vibration. The increase in contact stiffness due to wear and continuous rubbing is about 35% of its initial established value which correspond to an increase of squeal frequency by about 8%. Also, the relative sliding speed may change the squeal frequency due to wear of contacting surfaces which cause the variation of contact stiffness.

7. References

[1] **Sinclair, D., and Manville, N.J.,** "Frictional Vibrations", *ASME Journal of Applied Mechanics*, (1955), pp. 207-213.

[2] **Fosberry, R.A.C., and Holubecki, Z.,** "Disc Brake Squeal, its Mechanism and Suppression", *M.I.R.A. Research Report No. 1961/2*, (1961).

[3] **Spurr, R.T.,** "A Theory of Brake Squeal", *Proccedings of the Automotive Division, Inst. Mech. Engineers (AD)*, No. 1, (1961), pp. 33-40.

[4] **Tondl, A.,** "Quenching Of Self-Excited Vibrations:Equilibrium Aspects", Journal of Sound & vibrations, Vol. 42, (1975), pp. 251-260.

[5] **Rhee, S.K., Tsang, H.S., and Wang, Y.S.,** "Friction Induced Noise And Vibration Of Disc Brakes", *Wear*, (1989), Vol. 133, pp. 39-45.

[6] **Jarvis, R., and Mills, B.,** "Vibration Induced by Dry Friction", *Proccedings of Instit. Mech. Engineers*, Vol. 178, No. 32, (1963), pp.847-866.

[7] **Dweib, A.H., and D'Souza, A.F.,** "Self-Excited Vibrations Induced By Dry Friction, Part 1: Experimental Study", *Journal of Sound and Vibration*, Vol. 137, No. 2, (1990), pp. 163-175.

[8] **Millner, N., "An Analysis of Disc Brake Squeal**," *SAE Technical Paper 780332, doi:10.4271/780332*, (1978).

[9] **Earles, S.W.E., and Lee, C.K.,** "Instabilities Arising from the Frictional Interaction of a Pin-Disk System Resulting in Noise Generation", *ASME J. Eng. For Industry*, Vol. 98, (1976), pp. 81-86.

[10] **Okamura, H., and Ikeuchi, T.,** "Study on Disc Brake Squeal", *SAE paper 890864*, (1980).

[11] **Ibrahim, R.A.,** "Friction-Induced Vibration, Chatter, Squeal and Chaos Part II: Dynamics and Modeling", *Applied Mechanics Reviews*, Vol. 47, No. 7, (1994), *ASME Reprints No. AMR147*, pp. 227-253.

[12] **Watari, A., and Sugimoto, T.,** "Vibrations Caused by Dry Friction", *Bulletin of JSME*, Vol. 7, No. 25, (1964). pp. 40-52.

[13] **Antoniou, S.S.,** Cameron, A., and Gentle, C.R., "The Friction-Speed Relation from Stick-Slip Data", *Wear*, (1976), Vol. 36, pp. 235-254.

[14] **Basford, P.R., and Twiss, S.B.,** "Properties of Friction Materials I- Experiments on Variables Affecting Noise", *ASME Trans. 80*, (1958)a, pp. 402-406.

[15] **Basford, P.R., and Twiss, S.B.,** "Properties of Friction Materials II- Theory Of Vibrations in Brakes", *ASME Trans. 80*, (1958)b, pp. 407-4011.

[16] **Ibrahim, R.A**.,"Friction-Induced Vibration, Chatter, Squeal and Chaos Part I: Mechanics of Contact and Friction", *ASME Reprints No. AMR147, Applied Mechanics Reviews*, Vol. 47, No. 7, (1994), pp. 209-226.

[17] **Agrawal, O.P., Haug, E.J., and Wehage, R.A.,** "Some Friction Models for Dynamic Analysis of Mechanical Systems, Centre for Computer Aided Design", *Tech. Report University of Iowa* , No. 81-10, (1982).

[18] **Nakai, N., and Yokoi, M.,** "Generation Mechanism of Friction Noises in Dry Friction", *Japan Journal of Tribology*, Vol. 35, No. 5, (1990), pp. 513-522.

[19] **Hoffmann, N., and Gaul, L.,** "Effects of Damping on Mode-Coupling Instability in Friction Induced Oscillations", *ZAMM, Journal of Applied Mathematics and Mechanics, DOI: 10.1002/zamm.200310022*, Vol. 83, No. 8, (2003), pp. 524-534.

[20] **Giannini, O., and Sestieri, A.,** "Predictive Model of Squeal Noise Occurring on a Laboratory Brake", *Journal of Sound and Vibration 296*, (2006), pp. 583-601.

[21] **Huang, J.C., Krousgrill, C.M., and Bajaj, A.K.,** "An Efficient Approach To Estimate Critical Value of Friction Coefficient in Brake Squeal Analysis", *Transactions of the ASME, Journal of Applied Mechanics*, Vol. 74, No. 3, (2007), pp. 534-541.

[22] **Felske, A., Hoppe, G., and Matthai, M.,** "Oscillations in Squealing Disc Brakes-Analysis of Vibration Modes by Holographic Interferometry", *SAE paper 780333*.

[23] **Yang, M.M.,** "A System Study of Brake Rotor Modal Patterns", *Bosch Technical Report # EDB4-9066* (September 22, 1999), pp. 18-24.

[24] **Sherif, H.A.,** "Effect of Contact Stiffness on the Establishment of Self-Excited Vibrations", *Wear*, (1991), Vol. 141, pp. 227-234.

[25] **Nakai, N., and Yokoi M.,** "Generation Mechanism of Friction Noises in Dry Friction", *Japan Journal of Tribology*, Vol. 35, No. 5, (1990), pp. 513-522.

[26] **Eriksson, M., Bergman, F., and Jacobson, S.,** "Influence of Disk Topography on Generation of Brake Squeal", *Wear*, (1999), Vol. 225, pp. 621-633.

[27] **Eriksson, M., Bergman, F., and Jacobson, S.,** "Surface Characterization of Brake Pads After Running Under Silent and Squealing Conditions", *Wear*, (1999), Vol. 232, pp. 163-167.

[28] **Sherif, H.A.,** "Investigation on Effect of Surface Topography of Pad/Disc Assembly on Squeal Generation", *Wear*, (2004), pp. 687-695.

[29] **Sinou, J.J., and Jezequel L.,** "Mode Coupling Instability in Friction-Induced Vibrations and Its Dependency on System Parameters Including Damping", *European Journal of Mechanics A, Solids 26*, (2007), pp. 106-122.

[30] **Duffour, P., and Woodhouse, J.,** "Instability of Systems With a Frictional Point Contact.vPart3:vExperimental Tests", *Journal of Sound and Vibration 304* (2007), pp. 186–200.

[31] **Emira, M.N.A.,** "Friction-Induced Oscillations of a Slider:Parametric Study of Some System Parameters", *Journal of Sound and Vibration 300*, (2007), pp. 916–931.

[32] **Wagner, U. V., Hochlenert, D., and Hagedorn P.,** "Minimal Models for Disk Brake Squeal", *Journal of Sound and Vibration 302*, (2007), pp. 527–539.

[33] **Butlin, T., and Woodhouse J.,** "Sensitivity of Friction-Induced Vibration in Idealised Systems", *Journal of Sound and Vibration 319*, (2009), pp. 182–198.

[34] **Duffour, P., and Woodhouse, J.,** "Instability of Systems With a Frictional Point Contact. PART 1: BASIC MODELLING", *Journal of Sound and Vibration 271* (2004), pp. 365–390.

[35] **Butlin, T., and Woodhouse, J.,** "Friction-Inducedvibration: Should Low-Order Models be Believed? ", *Journal of Sound and Vibration 328*, (2009), pp. 92–108

[36] **Thomas, T.R., and Sayles R.S.,** "Stiffness of Machine Tool Joints: a Random-Process Approach", *Trans. Am. Soc. Mech. Eng., Journal of Eng. Ind*., (1979), Vol. 99, pp. 250-254.

[37] **Sherif, H.A**.," Parameters Affecting Contact Stiffness of Nominally Flat Surfaces", *Wear*, (1991), Vol. 145, pp. 113-121.

[38] **Sherif, H.A., and Kossa, S.S.,** "Relationship Between Normal and Tangential Contact Stiffness of Nominally Flat Surfaces", *Wear*, (1999), Vol. 151, pp. 49-62.

[39] **Cretegny, J.F.,** *Etude Theorique Et Experimentale Des Raideurs De Contact*, Saint-Ouen, France, DDI Thesis ISMCM, 1985.

[40] **McLeod, A.J., and Bishop, R.E.D.,** *The Forced Vibration Of Circular Flat Plates*, Great Britain, Mechanical engineering science monograph, Institution of Mechanical Engineers 1965.

الاهتزازات المستثارة ذاتياً الناتجة من التداخل الديناميكي مع ترايبولوجيا الاسطح

هاني على شريف وعبدالرحيم عماد

كلية الهندسة، جامعة القصيم، بريدة، المملكة العربية السعودية

hasherif@qec.edu.sa

)قدم للنشر في 1121/1/12 م؛ وقبل للنشر في 1122/5/21 م(

ملخص البحث. يقدم هذا البحث نموذج مرن لنظام حشوة الفرامل الواقعة تحت تأثير الاحتكاك مع القرص الدوار في الفرامل ذات القرص. هذا النموذج قد يعطي بعض النفسيرات حول ظاهرة الاهتزازات المستثارة الذاتية الناجمة عن الاحتكاك اجلاف المستمر. واعتمادًا على هذا النموذج، فإنه ميكن توضيح ان نشأة واستمرار الاهتزازات المستثارة الذاتية في نظام الفرامل مرتبط إلى خصائص أسطح النالمس نضال عن اخلصائص الفيزيائية لمكونات منظومة الفرامل. وقد أظهر التحليل النظري والتجريبي أن الاهتزازات المستثارة الذاتية نلطلق عندما يقترب نرددها من نرددات الرنين اخلاصة حبشوة الفرامل أو القرص واليت مت حتويرها بسبب صالبة النالمس. وقد أظهرت المالحظة التجريبية أيضا أن هذه الصالبة نزيد بانسبة نصل الى25 ٪ من قيمنها الأولية أثناء حدوث الاهتزازات المستثارة الذاتية وذلك بسبب التآكل والنزالق المستمر.

واحدة من النتائج الرئيسية في هذا البحث ، هو أن حدوث الرنين ألي من نرددات النظام أصبح مرتبطاً في الأساس بقيمة صالبة النالمس اليت نتحور بسبب عملية التآكل المستمر حتت تأثير الاحمال وسرعات النزالق المختلفة. أيضا، أظهر البحث أن هناك حدود لنرددات الاهتزازات المستثارة ذاتياً واليت بعدها إما أن الاهتزازات المستثارة الذاتية تكون مستمرة أو أن نتنقل الى نوع آخر من هذه الاهتزازات المستثارة الذاتية. وقد يؤدي النغيير المفاجئ للنحميل أو لسرعة النزالق لتغيير وضع نردد الاهتزازات المستثارة الذاتية وحتولها الى نظام اهتزازات آخر.

9M ifx ¬mx gë

àı¿ı ➢kzœi

llyœ âı¿ıkLgIQus ½ržx âşmşs.rx uaL¿ı,ı، nmLL_ıkم9ım ı âşmzsgı م9ı2rx uLaau çşQ ¼ Lgş,LZ ı ã2aLÇı 3zx- ya ½iTLşrx ج LSSş .us Çş âı¿ı ➢zgs

- nmLL_ı âmzsœ
- nmLL_ıم9ım
- uLa9ı2zx ışÇ9›9szz
- uLa9ı2zx @az
- âşmLmáı âşmzsgı م9ı2›x

- âşsiş.gz›x ãmzsgı
- âşszzx ãmzsgı
- ãşzşzLzşzx ãmzsgı
- ãşsLşQşz›x ãmzsgı
- لyyşı ı yşz2s›x ãmzsœ

llàı¿ık àzr

Kâşyşı÷aık ãzIRLş u92şrx âı¿ı 3şÃs

ll.usır àı¿ık ıøışãs ½žrx ¬mQZx E i

J١ Kعٍ.AF 9au لLa ¼ âA.2QIrıźşzş aşaş E½âr9zx غF ar9QIr 3şQs 3QM 9œ ı u2şrx

J٢ Kòyşqszx âşQı2rx 3sLm.rx ı ½2a ›zşa ¼ Lœ.us Qşm ½žrx lœ9ñ ı nszrx ı u92şır yısı2srx ı yzâsrx ض.2rx لyLSSS ı lâş2ş.zx ârLãzx

K£ şsãs £ âşşas y9ñ òyaA ârLãa lE½ãs Qşı2sF òyaãrx ârLãzx

J٣ kع.xyzax ux,ı.ş ı òyşQszx âşQı2rx ux,Lzşşax

J٤

J٥ kyiş ,xyÃx غ yQIm ys, غ ò.zA ض.m لyLSSS ı uymx.zx

J٦ nszrx ux›Lãssx

ll.usrx ط.u Eç

J١ Kç9ımãx ò›9ş ãzırx â2α ı ٥L÷ax âaym ı âşQı2rx âşşgszx ı ,Lzşşax ı ârLαãLş £ QMSa u2şrx ن9zş ن

J٢ Kç.zs âgç .usır مzÃ غ ٥.us Qşm zÃ u2şrx ن9zş a ن

J٣ K@şz2sır â2αLz âı¿ık ¼ .usır âazãzx u92şrx çşQ

ll.usrx uIQşI2s Eج

llysãx ط yuş .usır u2şrx @şzãs zsm

J١ kuymx.qır ys ı yzrax ن9s2rx aşA ,α9ş ı ›aiş .usş £ şıa uTLşrx مzãş ن

J٢ K.ş.2srx ,şs, ya yşLsm ن›iş aş ç.zs âm9şaa ys ¼ âı¿ık uLşs .us ٥›Lmş ,9u a

J٣ ã.şş.2rx ½szırLş 9.zıa 2rz.m ı›uy.mx.zx ò.ãA ¼ ,9mz.zx ys ı yzrax ن9.s2rx ..ım ys ı yzrax z,şyrx Q.ş..a y.m âşyşı÷ax ã.zırış aiş u.TLşrx 3.m.ş

Kãqım ٠٠٢ ym asLQım zşys a uşş âşyşı÷ax ı

J٤ K.amãx ½ş aas ı ãALma ».s ça ،yzx âşLsm ¼ font 12 Times New Roman مzzsmş ı (Microsoft word) ¿aLs.ş

J٥ KA٤ @şT â2âα ٠٢ ym لyxzÇx ı uLa9m.rx yaLu u2şrx uL2âα ›zm zşyş as nu

J٦ Kâıãsma Çyãx â2âarx . ım Lgş 3Q2ş ½žrx âgÇx ı yQı2rx aşâr ı asx9sm ı uTLşrx @mx ı u2şrx ن9sm nszş ن

J٧ KLgıâms â2âα 3M yax9œ çα9s

J٨ Ku2şrx .ziş Q2ış س.gA ¼ ñşis ı Lœ.m› 3mIms nMT مLÃ,ãLş yzx 3zx- çşx.zx Çş ,Luş

½2ş.a ½.m9Ã 3.zx- aQÃ, .mzş çş.zx szşşA çşx.zx ãQsLã ¼ Las K.amrx Ç9sma .ım â2ş.a س›9Ãs 3zx- مLÃ,iş yzx ¼ Lgşrş ,Luş luLş,yzrx Es

.u.srx ãsMA ›z2rx @Ã.A ،zı¿ık @A.A Eaz asñF âş,yzrx @MLA E9şass ½aym ½şF u2şrx ن9s2A Lgsx,Laszx ı Çyãx ,L@ãx @i ar9zx ãıslm @MLs

Kuı2âarx مLÃ,s @i E½m9Ã ½şF

١ع ،٦١ م ،92m 2 ızx â2aLş ،Çı›ãx âşım âıa ?KLgsLœL÷ı LgQşT âş-92m.rx âşş.2rx ãzıQzx ¼ âşızızrx ò.şgı? Kaızşm @şœ.şş ،yzşQLx llJLia

K١٥١–١٠١ ،Eم٢٠٠٢F

3.zx- çş.zx @Ã, nszşA çşx.zx ãQsLã ¼ Las Ki٦١ ص ،٨٧ 2.rز لJLia ،uL2âarx ..mذ ça ½2ş..a ½.m9Ã 3.zx- y.zx ¼ Lgşrş ,Lu.ş lln.szrx Eç

K.usrx ãsMA .uLsrx @i .usrx ı›LzQA Eaz asñF Çlszrx ن9s2A Lgsx,Laszx ı Çyãx ,L@ãx @i ar9zx ãıslm @MLş £ m9şsa ½2ş.a ½2m9Ã

Kم٨٨٩١ ،ñmA ı¿r âşıœãx çş Laz llض.ı.rx ،âşãşşas ı ş.as âmx ،ذ llymşsrx nı÷ âãuzx K ı›Lqşım çLα ،am9şrx llJLia

K3Ãsma aıa ¼ u2şrLş ããı2szx م9m.rx ı ,9arx çşQ QA.s

K@m.rx ñ ñ ن9s2ş @m.rx ı لyzÇx ق9A ن9s2ş ı لyzÇx ن9s2ş ı u2şrx @şÃ.s ym ÿ âsma £ QşÃ.s uLa9m.rx ı لyzÇx @Ã.s

J١٠

K.usş @ غ .us ,x9m aşTLα Çş u2şrx ›L2ş a

K,9uszx aiş ya âısma yş.um ı âı¿ık ya ½szms uTLşrx .a2ş

K Jz2ş @ La 3ş12s ça ،½QzzK .ş,Lâs ¼ Lgşım ص9aszx uyşz2srx ,x.şş uTLşrx م9ıış

Kãa Lgşâr9a ¿sLSS ı ,x,ı ym âı¿ık ¼ ò,9uszx ›x9zx y2s

âımx.zx yş,ısm

E-mail: quecjour@qec.edu.sa